

Distributed Arithmetic Coding for the Asymmetric Slepian-Wolf problem

Marco Grangetto, *Member, IEEE*, Enrico Magli, *Senior Member, IEEE*, Gabriella Olmo, *Senior Member, IEEE*

EDICS: SEN-DCSC, SPC-CODC

Abstract

Distributed source coding schemes are typically based on the use of channels codes as source codes. In this paper we propose a new paradigm, termed “distributed arithmetic coding”, which exploits the fact that arithmetic codes are good source as well as channel codes. In particular, we propose a distributed binary arithmetic coder for Slepian-Wolf coding with decoder side information, along with a soft joint decoder. The proposed scheme provides several advantages over existing Slepian-Wolf coders, especially its good performance at small block lengths, and the ability to incorporate arbitrary source models in the encoding process, e.g. context-based statistical models. We have compared the performance of distributed arithmetic coding with turbo codes and low-density parity-check codes, and found that the proposed approach has very competitive performance.

Index Terms

Distributed source coding, arithmetic coding, Slepian-Wolf coding, Wyner-Ziv coding, compression.

M. Grangetto is with Dip. di Informatica, Università degli Studi di Torino, Corso Svizzera 185 - 10149 Torino - ITALY - Ph.: +39-011-6706711 - FAX: +39-011-751603 - E-mail: marco.grangetto@di.unito.it

E. Magli and G. Olmo are with Dip. di Elettronica, Politecnico di Torino, Corso Duca degli Abruzzi 24 - 10129 Torino - Italy - Ph.: +39-011-5644195 - FAX: +39-011-5644099 - E-mail: enrico.magli (gabriella.olmo)@polito.it.
Corresponding author: Enrico Magli.

Distributed Arithmetic Coding for the Asymmetric Slepian-Wolf problem

I. INTRODUCTION AND BACKGROUND

In recent years, distributed source coding (DSC) has received an increasing attention from the signal processing community. DSC considers a situation in which two (or more) statistically dependent data sources must be encoded by separate encoders that are not allowed to talk to each other. Performing separate lossless compression may seem less efficient than joint encoding; however, DSC theory proves that, under certain assumptions, separate encoding is optimal, provided that the sources are decoded jointly [1]. For example, with two sources it is possible to perform “standard” encoding of the first source (called *side information*) at a rate equal to its entropy, and “conditional” encoding of the second one at a rate lower than its entropy, with no information about the first source available at the second encoder; we refer to this as “asymmetric” Slepian-Wolf (S-W) problem. DSC theory also encompasses lossy compression [2]; it has been shown that, under certain conditions, there is no performance loss in using DSC [2], [3], and that possible losses are bounded below 0.5 bit per sample (bps) for quadratic distortion metric [4]. In practice, lossy DSC is typically implemented using a quantizer followed by lossless DSC, while the decoder consists of the joint entropy decoder followed by a joint dequantizer. Lossless and lossy DSC have several potential applications. e.g. coding for non co-located sources such as sensor networks, distributed video coding [5], [6], [7], [8], layered video coding [9], [10], error resilient video coding [11], and satellite image coding [12], [13], just to mention a few. The interested reader is referred to [14] for an excellent tutorial.

Traditional entropy coding of an information source can be performed using one out of many available methods, the most popular being arithmetic coding (AC) and Huffman coding. “Conditional” (i.e., DSC) coders are typically implemented using channel codes, by representing the source using the syndrome (or the parity bits) of a suitable channel code of given rate. The rationale of this approach is that channel codes often provide geometrical structures with maximum distance properties, so that decoding an ambiguous description of a source at a rate less than its entropy (given the side information) incurs minimum error probability.

Regarding asymmetric S-W coding, the first practical S-W coding technique has been described in [15], and employs trellis channel codes. Recently, more powerful channel codes such as turbo codes have been proposed in [6], [16], [17], and low-density parity-check (LDPC) [18] codes have been used in [19], [20], [21]. Turbo and LDPC codes can get extremely close to channel capacity,

although they require the block size to be rather large. Note that the constituent codes of turbo-codes are convolutional codes, hence the syndrome is difficult to compute. In [6] the cosets are formed by all messages that produce the *same parity bits*, even though this approach is somewhat suboptimal [17], as these cosets do not have as good geometrical properties as those of syndrome-based coding. In [22] a syndrome former is used to address this problem. Multilevel codes have also be addressed; in [23] trellis codes are extended to multilevel sources, whereas in [24] a similar approach is proposed for LDPC codes.

Besides techniques based on channel coding, a few authors have also investigated the use of source coders for DSC. This is motivated by the fact that existing source coders obviously exhibit nice compression features that should be retained in a DSC coder, such as the ability to employ flexible and adaptive probability models, and low encoding complexity. In [25] the problem of designing a variable-length DSC coder is addressed; it is shown that the problem of designing a zero-error such coder is NP-hard. In [26] a similar approach is followed; the authors consider the problem of designing Huffman and arithmetic DSC coders for multilevel sources with zero or almost-zero error probability. The idea is that, if the joint density of the source and the side information satisfies certain conditions, the same codeword (or the same interval for the AC process) can be associated to multiple symbols. This approach leads to an encoder with a complex modeling stage (NP-hard for the optimal code, though suboptimal polynomial-time algorithms are provided in [26]), while the decoding process resembles a classical arithmetic decoder.

Although several near-capacity DSC coders have been designed for simple ideal sources (e.g., binary and Gaussian sources), the applications of practical DSC schemes to realistic signals typically incurs the following problems.

- Capacity-achieving channel codes require very large data blocks (typically in excess of 10^5 symbols). This requirement is often not compatible with practical applications, where the basic units to be encoded are of the order of a few hundreds to a few thousands symbols.
- The symbols contained in a block are expected to follow a stationary statistical distribution. However, typical real-world sources are not stationary; this calls for either the use of short blocks, which weakens the performance of the S-W coder, or the estimation of conditional probabilities over contexts, which cannot be accommodated by existing S-W coders.
- When the sources are very correlated (i.e., in the most favorable case), very high-rate channel codes are needed (e.g., rate- $\frac{99}{100}$ codes). However, capacity-achieving channel codes are often not very efficient at high rate.
- In those applications where DSC is used to limit the encoder complexity, it should be noted that the complexity of existing S-W coders is not negligible, and often higher than that of existing

non-DSC coders. This seriously weakens the benefits of DSC.

- Upgrading an existing compression algorithm like JPEG 2000 or H.264/AVC in order to provide DSC functionalities requires at least to redesign the entropy coding stage, adopting one of the existing DSC schemes.

Among these issues, the block length is particularly important. While it has been shown that, on ideal sources with very large block length, the performance of some practical DSC coders can be as close as 0.09 bits to the theoretical limit [14], so far DSC of real-world data has fallen short of its expectations, one reason being the necessity to employ much smaller blocks. For example, the PRISM video coder [5] encodes each macroblock independently, with a block length of 256 samples; for the coder in [6], the block length is equal to the number of 8x8 blocks in one picture (1584 for the CIF format). The performance of both coders is rather far from optimal, highlighting the need for DSC coders addressing realistic block lengths.

A solution to this problem has been introduced in [27], where an extension of AC, named distributed arithmetic coding (DAC), has been proposed for asymmetric S-W coding¹. DAC and its decoding process do not currently have a rigorous mathematical theory that proves they can asymptotically achieve the S-W rate region; such theory is very difficult to develop because of the non-linearity of AC. However, DAC is a practical algorithm that was shown in [27] to outperform other existing distributed coders. In this paper, we build on the results presented in [27], providing several new contributions. First, we generalize DAC to the encoding of binary sources with arbitrary and time-varying probability distribution; this allows to employ DAC in a wider set of applications, including context-based coding through the estimation of conditional probabilities. Second, we introduce and discuss an improved termination procedure for the DAC encoder. Third, we investigate the rate allocation problem for DAC, in terms of how to optimally select the encoding parameters to achieve a desired target rate with minimum decoder error probability. Finally, we evaluate the performance of this new design comparing it with turbo codes and LDPC codes. We also consider the case of extremely correlated sources with highly non-uniform probabilities; this is of interest in multimedia applications because the most significant bit-planes of the transform coefficients of an image or video sequence are almost always equal to zero, and are very correlated with the side information.

Interestingly, we have found that the DAC can be applied to highly non-uniform sources (i.e., when the two symbols have significantly skewed probability distribution), without any performance loss with respect to the uniform case, as opposed to turbo codes [29]. Finally, it should be noted that the DAC principle can also be used for symmetric S-W coding; preliminary results are shown

¹A similar scheme has been independently and concurrently developed in [28] using quasi-arithmetic codes.

in [30].

This paper is organized as follows. In Sect. IV we describe the DAC encoding process. In Sect. III we study the rate allocation and parameter selection problem. In Sect. IV we describe the DAC decoder. In Sect. V we report the results of a performance assessment of DAC, and in Sect. VI we draw some conclusions and outline possible research developments.

II. DISTRIBUTED ARITHMETIC CODING: ENCODER

Before describing the DAC encoder, it should be noted that the AC process typically consists of a modeling stage and a coding stage. The modeling stage has the purpose of computing the parameters of a suitable statistical model of the source, in terms of the probability that a given bit of the input sequence takes on value 0 or 1. This model can be arbitrarily sophisticated, e.g. by using contexts, adaptive probability estimation, and so forth. The coding stage takes the probabilities as input, and implements the actual AC procedure, which outputs a binary codeword describing the input source.

Let $\mathbf{X} = [X_0, X_1, \dots, X_i, \dots, X_{N-1}]$ be a length- N binary symbol sequence with probabilities $p_{i,0}^X = P(X_i = 0)$ and $p_{i,1}^X = P(X_i = 1)$, with $i = 0, \dots, N-1$. The dependence of the source probabilities on i emphasizes the fact that the sequence \mathbf{X} may be an occurrence of a nonstationary random process. The modeling and coding stages are shown in Fig. 1-a. The modeling stage takes as input the sequence \mathbf{X} , and outputs an estimate of the probabilities $p_{i,0}^X$ and $p_{i,1}^X$; the estimation process is typically causal, i.e. $p_{i,j}^X$ is estimated using samples X_0, \dots, X_{i-1} . The coding stage takes as input \mathbf{X} , $p_{i,0}^X$ and $p_{i,1}^X$, and generates a codeword \mathbf{C}_X . The average length of \mathbf{C}_X depends on $p_{i,0}^X$ and $p_{i,1}^X$, and is determined once these probabilities are given.

In order to use the DAC, we consider two sources \mathbf{X} and \mathbf{Y} , where $\mathbf{Y} = [Y_0, Y_1, \dots, Y_i, \dots, Y_{N-1}]$ is a length- N binary symbol sequence with probabilities $p_{i,0}^Y = P(Y_i = 0)$ and $p_{i,1}^Y = P(Y_i = 1)$, with $i = 0, \dots, N-1$. We also assume that X_i and Y_i are statistically dependent. For DAC, three blocks can be identified, as in Fig. 1-b, namely the modeling, rate allocation, and coding stages. The modeling stage is exactly the same as for the classical AC. The coding stage will be described in Sect. II-B; it takes as inputs \mathbf{X} , the probabilities $p_{i,0}^X$ and $p_{i,1}^X$, and a set of parameters k_i^X , and outputs a codeword \mathbf{C}'_X . In addition, we also have a rate allocation stage that selects the target average rate of the codeword \mathbf{C}'_X . Unlike a classical AC, where the average rate is function of the source probabilities, and hence cannot be selected *a priori*, the DAC allows to select any desired bit-rate not larger than the average rate of a classical AC. This is very important, since in a DSC setting the bit-rate for \mathbf{X} should depend not only on how much “compressible” the source is (e.g., if $p_{i,0}^X \gg p_{i,1}^X$, or $p_{i,0}^X \simeq p_{i,1}^X$), but also on how much correlated X_i and Y_i are. For this reason, the rate allocator takes as input the probabilities $p_{i,0}^X$ and $p_{i,1}^X$, the conditional entropies $H(X_i|Y_i)$, and

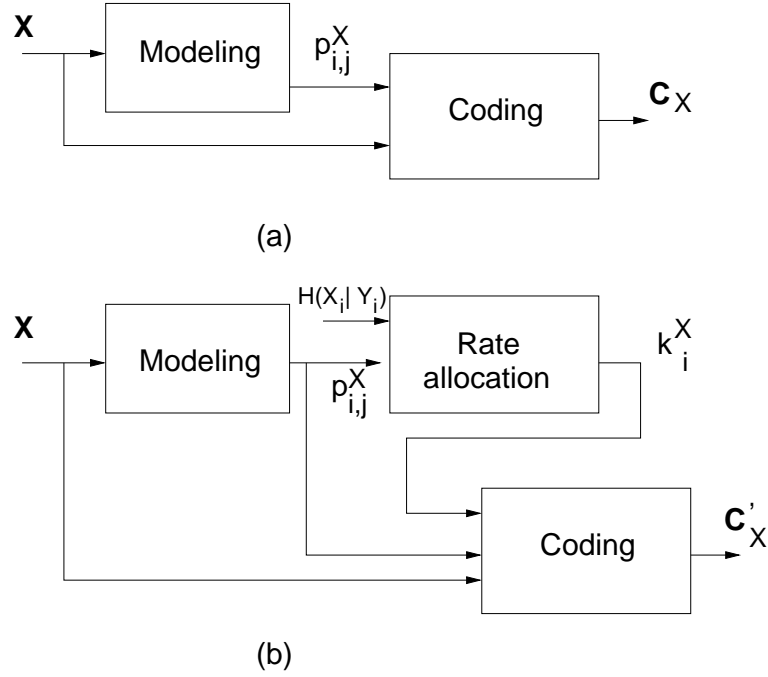


Fig. 1. Modeling, rate allocation and coding stage for (a) classical AC, and (b) DAC.

outputs a set of parameters k_i^X that will drive the DAC coding stage to achieve the desired rate. In Sect. III we show how the rate allocation can be performed with a few simple statistical models.

In this paper we deal with the coding and rate allocation stages, and assume that the input probabilities $p_{i,0}^X$, $p_{i,1}^X$ and conditional entropy $H(X_i|Y_i)$ are known *a priori*. This allows us to focus on the distributed coding aspects of the proposed scheme, and, at the same time, keeps the scheme independent of the modeling stage, so that any such stage can be applied to the DAC, e.g. a context-based probability model, feeding the AC process with conditional probabilities that are different for each input bit. Therefore, from now on, we will assume that the input probabilities are known.

A. Arithmetic coding

We first review the classical AC coding process, as this sets the stage for the description of the DAC encoder. The binary AC process for \mathbf{X} is based on the probabilities $p_{i,0}^X$ and $p_{i,1}^X$, which are used to partition the $[0, 1)$ interval into sub-intervals associated to possible occurrences of the source symbols. At initialization the “current” interval I_0 is set to $I_0 = [0, 1)$. For each input symbol X_i , the current interval I_i is partitioned into two adjacent sub-intervals whose lengths are proportional to $p_{i,0}^X$ and $p_{i,1}^X$. The sub-interval corresponding to the actual value of symbol X_i is selected as the next current interval I_{i+1} , and this procedure is repeated for the next symbol. After all N symbols have been processed, the sequence is represented by the final interval I_N . The codeword \mathbf{C}_X can consist

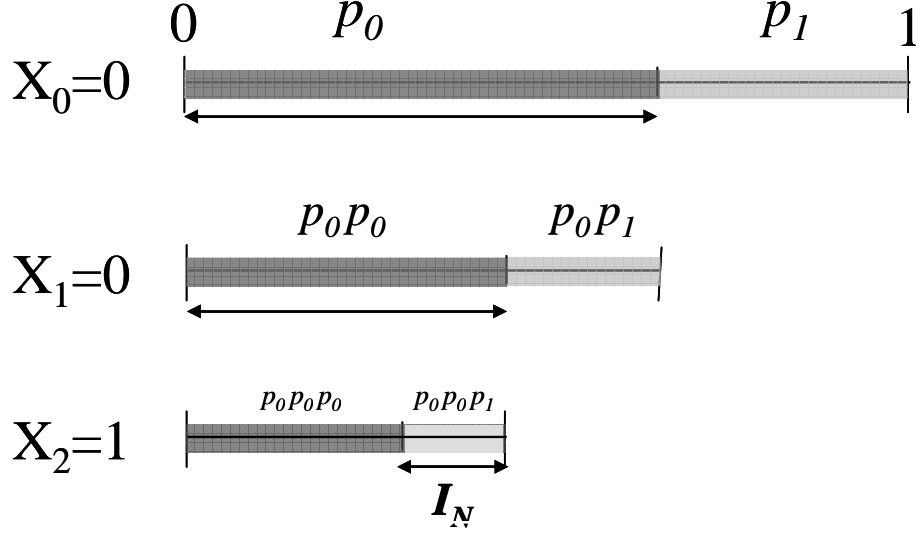


Fig. 2. Encoding procedure for three symbols using a binary AC.

in the fractional part of the binary representation of any number inside I_N (e.g., the mid-point, the lowest endpoint, or the shortest number in I_N), and requires approximately $-\log_2 |I_N|$ bits, where $|I_N|$ is the amplitude of I_N .

As an example, consider the drawing in Fig. 2, where a binary AC encodes a string of $N = 3$ symbols $\mathbf{X} = [0 \ 0 \ 1]$. The figure shows the interval lengths at each step of the encoding process, as well as the final interval I_N . The probabilities $p_{i,0}^X$ and $p_{i,1}^X$ are also reported, using the simplified notation p_0 and p_1 .

B. DAC encoder

The encoder can be used for both asymmetric and symmetric DSC. In the asymmetric case, which is considered in this paper, \mathbf{X} is coded using a DAC, and the side information \mathbf{Y} is assumed to be available at the decoder. The source \mathbf{X} is encoded using a DAC at a certain coding rate R'_X , not less than $H(\mathbf{X}|\mathbf{Y})$; the problem of how to select the DAC coding parameters to achieve the target rate R'_X is discussed in Sect. III. The codeword \mathbf{C}'_X generated by the DAC is communicated to the decoder, which can then perform joint decoding as described in Sect. IV. While AC provides a complete description of the input string \mathbf{X} , the DAC provides a lower-rate incomplete description that cannot be decoded exactly in absence of a side information \mathbf{Y} .

Similarly to other S-W coders, DAC is based on the principle of inserting some ambiguity in the source description during the encoding process. This is obtained using a modified interval subdivision strategy; in particular, the DAC employs a set of intervals whose amplitudes are proportional to the modified probabilities $\tilde{p}_{i,0}^X$ and $\tilde{p}_{i,1}^X$, such that $\tilde{p}_{i,0}^X \geq p_{i,0}^X$ and $\tilde{p}_{i,1}^X \geq p_{i,1}^X$. In order to fit the enlarged

sub-intervals into the $[0, 1)$ interval, the sub-intervals are allowed to partially overlap. For example, at initialization the current interval is set to $[0, 1)$; if the interval for symbol “0” precedes that for symbol “1”, the two subintervals for classical AC would be $[0, p_{i,0}^X)$ and $[p_{i,0}^X, 1)$; instead, the subintervals for DAC are taken as $[0, \tilde{p}_{i,0}^X)$ and $[1 - \tilde{p}_{i,1}^X, 1)$. The intuition behind this process is that, since $1 - \tilde{p}_{i,1}^X \leq \tilde{p}_{i,0}^X$, the intervals are generally not disjoint. Therefore, since the received codeword does not generally allow the decoder to select one out the two intervals at time i , unambiguous decoding is not possible without additional information.

The detailed DAC encoding procedure is described in the following. At initialization the “current” interval I'_0 is set to $I'_0 = [0, 1)$. For each input symbol X_i , the current interval I'_i is subdivided into two partially overlapped sub-intervals whose lengths are proportional to $\tilde{p}_{i,0}^X$ and $\tilde{p}_{i,1}^X$. The interval representing the symbol X_i is selected as the next current interval I'_{i+1} . After all N symbols have been processed, the sequence is represented by the final interval I'_N ; the codeword C'_X can consist in the fractional part of the binary representation of any number inside I'_N , and requires approximately $-\log_2 |I'_N|$ bits. This procedure is sketched in Fig. 3 using the simplified notation \tilde{p}_0 and \tilde{p}_1 ; at the decoder side, whenever the codeword points to an overlapped region, the source symbol cannot be detected unambiguously, and additional information must be exploited by the joint decoder to solve the ambiguity.

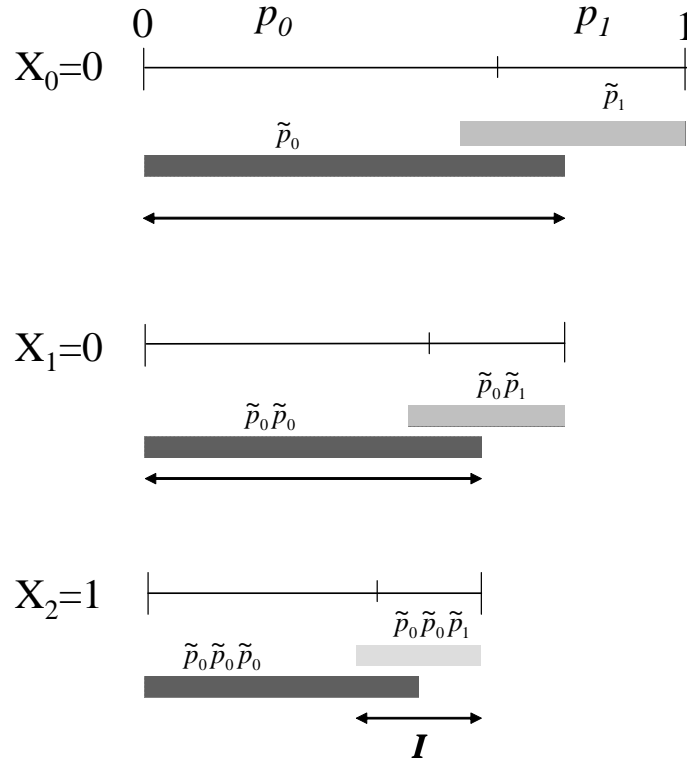


Fig. 3. Distributed arithmetic encoding procedure.

It is worth noticing that the DAC encoding procedure is a generalization of AC. As a matter of fact, setting $\tilde{p}_{i,0}^X = p_{i,0}^X$ and $\tilde{p}_{i,1}^X = p_{i,1}^X$ for all i yields the AC encoding process described in Sect. II-A, with $I'_N = I_N$ and $\mathbf{C}'_X = \mathbf{C}_X$. In general, when $\tilde{p}_{i,0}^X > p_{i,0}^X$ and $\tilde{p}_{i,1}^X > p_{i,1}^X$, the intervals are larger, so that $|I'_N| > |I_N|$; as a consequence, the codeword \mathbf{C}'_X is shorter than \mathbf{C}_X , to an extent that depends on the amount of overlap. This is consistent with the notion that an ambiguous description of a source requires less bits than a complete description, and provides the further compression warranted by DSC.

It should also be noted that, for simplicity, the description of the AC and DAC provided above assumes infinite precision arithmetic. While we have described an ideal DAC, its practical implementation needs to employ a few technicalities, such as interval renormalization, approximations of the unit interval, and so on, to speed up the encoding and decoding process, as well as to operate in finite precision arithmetic.

III. RATE ALLOCATION AND CHOICE OF THE OVERLAP FACTOR

The length of codeword \mathbf{C}'_X is determined by the length $|I'_N|$ of the final interval, which in turn depends on how much $\tilde{p}_{i,0}^X$ and $\tilde{p}_{i,1}^X$ are larger than $p_{i,0}^X$ and $p_{i,1}^X$. As a consequence, in order to select the desired rate, it is important to quantitatively determine how much the average rate depends on the overlap, because this will drive the selection of the desired amount of overlap. Moreover, we need to understand how to select the overlap in order to achieve good performance. In the following we derive the average bit-rate obtained by the DAC as a function of the set of input probabilities and the amount of overlap, and investigate how to select the proper overlap to obtain a given target bit-rate.

A. Definition of the rate allocation problem

The derivation of the average bit-rate uses the probabilities $p_{i,j}^X$, with $i = 0, \dots, N-1$ and $j = 0, 1$. As has been said, we do not make any assumptions on these probabilities; we assume that the modeling stage knows or estimates them, and passes them to the DAC rate allocation and encoding stages. We are interested in finding the average rate $\tilde{R}_k^l(\mathbf{X})$ that a DAC employs to describe the bits with index from k to l of the input sequence, with $0 \leq k \leq N-1$ and $k \leq l \leq N-1$. The total rate employed to describe \mathbf{X} is $\tilde{R}_0^{N-1}(\mathbf{X})$. The rate $\tilde{R}_k^l(\mathbf{X})$ is given by the following formula:

$$\tilde{R}_k^l(\mathbf{X}) = \frac{1}{l - k + 1} \sum_{i=k}^l \tilde{R}_i^i(\mathbf{X}) \quad (1)$$

where $\tilde{R}_i^i(\mathbf{X})$ is the average instantaneous rate used to encode the i -th input bit:

$$\tilde{R}_i^i(\mathbf{X}) = \sum_{j=0}^1 p_{i,j}^X \log_2 \frac{1}{\tilde{p}_{i,j}^X} \quad (2)$$

This can be derived straightforwardly from the property that the codeword generated by an AC has an average length that depends on the size of the final interval [31], that is, on the product of the probabilities $\tilde{p}_{i,j}^X$ at each instant i , and hence on the amount of overlap; the expectation is computed using the true probabilities $p_{i,j}^X$.

We set $\tilde{p}_{i,j}^X = \alpha_{i,j}^X p_{i,j}^X$, where $\alpha_{i,j}^X \geq 1$, so that $\tilde{p}_{i,0}^X + \tilde{p}_{i,1}^X \geq 1$. This amounts to enlarging each interval by an amount proportional to the overlap factors $\alpha_{i,j}^X$. The average coding rate achieved by the DAC becomes

$$\begin{aligned} \tilde{R}_k^l(\mathbf{X}) &= \frac{1}{l-k+1} \sum_{i=k}^l \sum_{j=0}^1 p_{i,j}^X \left(\log_2 \frac{1}{p_{i,j}^X} - \log_2 \alpha_{i,j}^X \right) = \\ &= \frac{1}{l-k+1} \sum_{i=k}^l \sum_{j=0}^1 p_{i,j}^X (r_{i,j}^X - \delta r_{i,j}^X) \end{aligned}$$

where $r_{i,j}^X = -\log_2 p_{i,j}^X$, and $\delta r_{i,j}^X = \log_2 \alpha_{i,j}^X$. Note that $r_{i,j}^X$ represents the rate contribution of symbol j at time i yielded by standard AC, while $\delta r_{i,j}^X$ represents the average decrease of this contribution, i.e. the average number of bits saved in the binary representation of the j -th input symbol at time i given by DAC.

B. Design of the overlap factors

The expression above reflects the intuitive concept that the average bit-rate depends on the amount of overlap between the intervals, and on how this overlap is distributed between them. In general, a large amount of overlap will lead to a larger final interval, and hence to a shorter codeword. Through proper selection of $\alpha_{i,j}^X$, this overlap can be assigned in various ways to symbols “0” and “1”. Hence, the problem arises of selecting suitable overlap factors $\alpha_{i,j}^X$. In particular, we state our design problem as selecting the set of $\alpha_{i,j}^X$ that are optimal under some criterion, given a constraint on the target bit-rate such that $\tilde{R}_k^l(\mathbf{X}) = R'_X$.

To address this problem, we can interpret the DAC encoder as is shown in Fig. 4. For simplicity, and without loss of generality, we drop the subscript i and consider a source \mathbf{X} with prior probabilities p_0^X and p_1^X , which define the intervals as shown in the top part of Fig. 4. The DAC uses overlapped intervals of size $\alpha_0^X p_0^X$ and $\alpha_1^X p_1^X$ respectively, as in the bottom part of Fig. 4. The codeword \mathbf{C}_X generated by an AC identifies input symbol 0 or 1 according to whether it is contained in the leftmost or rightmost interval; by construction, this happens with probability respectively p_0 and p_1 .

For the DAC, four different cases are possible; we consider these cases as the elements of the alphabet $\{0, A1, A0, 1\}$ of a new source \mathbf{Z} , and interpret the DAC as an M -ary AC, with $M = 4$. The statistical properties of this alphabet are given by the probabilities p_0^Z , p_{A0}^Z , p_{A1}^Z , and p_1^Z . Specifically, when a symbol of \mathbf{X} is equal to 0, the DAC outputs one out of the symbols 0, A1 and A0; the union

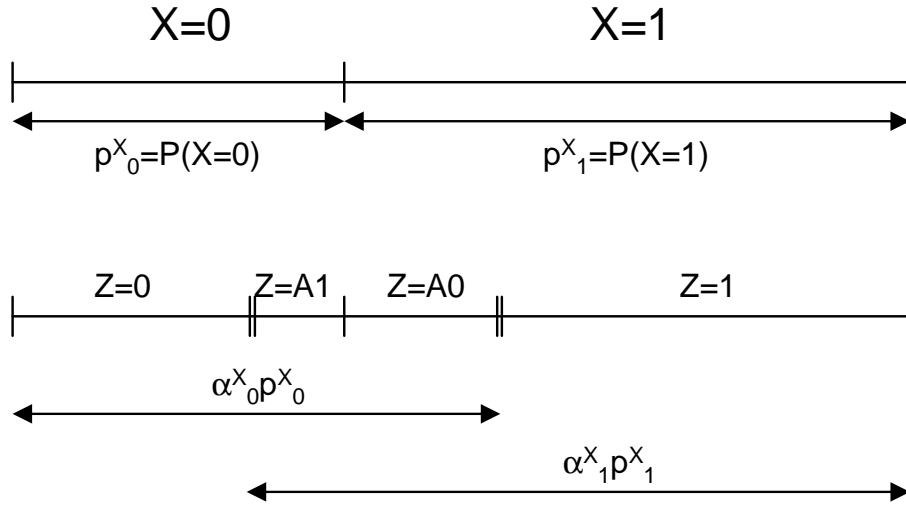


Fig. 4. DAC model as M -ary arithmetic coder. Top: classical AC; bottom: DAC.

of the intervals associated to 0, A1 and A0 is the interval of length $\alpha^X_0 p^X_0$ that the DAC associates to symbol 0. Similarly, when a symbol of \mathbf{X} is equal to 1, the DAC outputs one out of the symbols A1, A0 and 1.

The symbols A0 and A1 are “ambiguous” symbols that are selected when the codeword \mathbf{C}'_X lies in the overlapped portion of the intervals. From the decoder standpoint, given \mathbf{C}'_X , a classical binary arithmetic decoder will be unable to determine the original input sequence \mathbf{X} . The decoder may be able to decode some bits of \mathbf{X} , namely those bits where the codeword lies in a non-overlapped portion of either interval, corresponding to symbol 0 or 1 of \mathbf{Z} . However, oftentimes the codeword will fall in the overlapped portion, and the decoder will need to resort to the side information to disambiguate the symbol.

It is worth noting that, given \mathbf{C}'_X , a 4-ary arithmetic decoder can univocally determine the source \mathbf{Z} corresponding to that codeword; moreover, there is no other sequence $\mathbf{Z}^* \neq \mathbf{Z}$ that yields the same codeword \mathbf{C}'_X . It is hence evident that the source \mathbf{Z} carries as much information about \mathbf{X} as the codeword \mathbf{C}'_X . In other terms, the DAC generates a codeword \mathbf{C}'_X that describes \mathbf{X} ambiguously; the same codeword \mathbf{C}'_X univocally determines a sequence \mathbf{Z} , as the output of the arithmetic decoding process of \mathbf{C}'_X , using the intervals related to the probability distribution of \mathbf{Z} .

Nevertheless, one should not consider \mathbf{C}'_X as the codeword generated by an AC that encodes \mathbf{Z} . If this were the case, the average length of \mathbf{C}'_X would be approximately $H(\mathbf{Z})$; on the contrary, this length is approximately equal to $H(\mathbf{X})$, which is significantly smaller than $H(\mathbf{Z})$. The trick is that, when the DAC encodes \mathbf{X} , it does not *choose* symbols A0 and A1; rather, A0 and A1 are fictitious symbols generated as a by-product of the encoding process.

The design of the overlap factors should be done in such a way that the source \mathbf{Z} yielded by a 4-ary arithmetic decoder contains as much information as possible about \mathbf{X} , given a target bit-rate. To derive the statistical properties of \mathbf{Z} , we use the definition of the DAC. In particular, when the input symbol of \mathbf{X} is 0, the DAC chooses the interval that is the union of the intervals of 0, A1 and A0. If the codewords related to input symbol 0 of \mathbf{X} are uniformly distributed over the interval of length $\alpha_0^X p_0^X$, the probability of 0, A1 and A0 is proportional to the interval lengths. Similarly, when the input symbol of \mathbf{X} is 1, the DAC chooses the interval that is the union of the intervals of A1, A0 and 1, and the probability of these symbols is proportional to their interval length. Therefore, we obtain the following set of marginal probabilities for \mathbf{Z} : $p_0^Z = 1 - \alpha_1^X p_1^X$, $p_1^Z = 1 - \alpha_0^X p_0^X$, $p_{A0}^Z = p_1^X - (1 - \alpha_0^X p_0^X)$, $p_{A1}^Z = p_0^X - (1 - \alpha_1^X p_1^X)$. The joint probability distribution $p(\mathbf{X}, \mathbf{Z})$ can be written as follows.

$$\begin{aligned}
p(0, 0) &= P(\mathbf{Z} = 0 | \mathbf{X} = 0) P(\mathbf{X} = 0) \\
&= \frac{P(\mathbf{Z} = 0)}{P(\mathbf{Z} = 0) + P(\mathbf{Z} = A1) + P(\mathbf{Z} = A0)} P(\mathbf{X} = 0) = \frac{1 - \alpha_1^X p_1^X}{\alpha_0^X} \\
p(1, 0) &= 0 \\
p(0, 1) &= 0 \\
p(1, 1) &= \frac{P(\mathbf{Z} = 1)}{P(\mathbf{Z} = 1) + P(\mathbf{Z} = A1) + P(\mathbf{Z} = A0)} P(\mathbf{X} = 1) = \frac{1 - \alpha_0^X p_0^X}{\alpha_1^X} \\
p(0, A1) &= \frac{P(\mathbf{Z} = A1)}{P(\mathbf{Z} = 0) + P(\mathbf{Z} = A1) + P(\mathbf{Z} = A0)} P(\mathbf{X} = 1) = \frac{p_0^X - (1 - \alpha_1^X p_1^X)}{\alpha_0^X} \\
p(1, A1) &= \frac{P(\mathbf{Z} = A1)}{P(\mathbf{Z} = 1) + P(\mathbf{Z} = A1) + P(\mathbf{Z} = A0)} P(\mathbf{X} = 1) = \frac{p_0^X - (1 - \alpha_1^X p_1^X)}{\alpha_1^X} \\
p(0, A0) &= \frac{P(\mathbf{Z} = A0)}{P(\mathbf{Z} = 0) + P(\mathbf{Z} = A1) + P(\mathbf{Z} = A0)} P(\mathbf{X} = 0) = \frac{p_1^X - (1 - \alpha_0^X p_0^X)}{\alpha_0^X} \\
p(1, A0) &= \frac{P(\mathbf{Z} = A0)}{P(\mathbf{Z} = 1) + P(\mathbf{Z} = A1) + P(\mathbf{Z} = A0)} P(\mathbf{X} = 1) = \frac{p_1^X - (1 - \alpha_0^X p_0^X)}{\alpha_1^X}
\end{aligned}$$

The overlap factors α_0^X and α_1^X must maximize the mutual information $I(\mathbf{Z}; \mathbf{X})$, subject to the constraint that the average bit-rate is equal to R'_X . The mutual information can be written as $I(\mathbf{Z}; \mathbf{X}) = I(\mathbf{X}; \mathbf{Z}) = H(\mathbf{X}) - H(\mathbf{X} | \mathbf{Z})$. As a consequence, since $H(\mathbf{X})$ does not depend on the overlap factors, maximizing $I(\mathbf{Z}; \mathbf{X})$ amounts to minimizing $H(\mathbf{X} | \mathbf{Z})$. This conditional entropy can be computed using the joint and conditional distributions of \mathbf{X} and \mathbf{Z} , which are readily derived using the joint and marginal distributions given above. The computations, which are omitted for brevity, yield the following expression:

$$H(\mathbf{X} | \mathbf{Z}) = p_0^X \log_2 \alpha_0^X + p_1^X \log_2 \alpha_1^X \quad (3)$$

Letting $\alpha_0^X = \alpha_1^X = 1$, i.e. no overlap at all, yields that $H(\mathbf{X}|\mathbf{Z}) = 0$, and hence $I(\mathbf{Z}; \mathbf{X}) = H(\mathbf{X})$, confirming that this choice yields the classical lossless AC coding process.

Regarding the rate constraint, from (2) it can be seen that the rate R'_X can be written as

$$R'_X = -\sum_{j=0}^1 p_j^X \log_2(\alpha_j^X p_j^X) = -(p_0^X \log_2 \alpha_0^X + p_1^X \log_2 \alpha_1^X) + H(\mathbf{X}) \quad (4)$$

Comparing (3) and (4) shows that the constraint equation, which is a function of α_0^X and α_1^X , is “parallel” to the cost function. This implies that any choice of α_0^X and α_1^X , such that the target rate is met, will provide a codeword \mathbf{C}'_X containing the maximum possible amount of information about \mathbf{X} .

This result leaves a lot of freedom in the design of the DAC encoder, since the only constraint on the $\alpha_{i,j}^X$ is the rate constraint, i.e. we have one equation and two unknowns. In other terms, it is the total amount of overlap, and not how it is distributed over the symbols “0” and “1”, that determines $I(\mathbf{X}; \mathbf{Z})$. This result has also been confirmed by simulation; in Sect. V it will be shown that the DAC performance is actually independent of the specific choice of $\alpha_{i,j}^X$.

As an example, a possible choice is to take equal overlap factors $\alpha_0^X = \alpha_1^X = \alpha^X$. This implies that each interval is enlarged by a fixed percentage α^X , which does not depend on the source probability p_j^X . This choice leads to a target rate

$$R'_X = H(\mathbf{X}) - \log_2 \alpha^X \quad (5)$$

C. A practical interval design rule

While the example interval choice described above is intuitive, it is not devoid of problems. Indeed, in order to allow any rate to be chosen, we need to make sure that the enlarged intervals $[0, \alpha_0^X p_0^X)$ and $[1 - \alpha_1^X p_1^X, 1)$ are both contained inside the $[0, 1)$ interval, because the AC and DAC coding process is defined over this interval, and not outside. Therefore, we should make sure that the following conditions are met:

$$\begin{cases} \alpha_0^X p_0^X < 1 \\ \alpha_1^X p_1^X \leq 1 \end{cases} \quad (6)$$

It should be noted that choosing $\alpha_0^X = \alpha_1^X = \alpha^X$ may lead to intervals that lie outside of $[0, 1)$. For example, let us assume that the source probabilities are $p_0^X = 0.1$ and $p_1^X = 0.9$; taking $\alpha^X \geq 1/0.9$ will lead to an enlarged interval for symbol 1 that does not fit into $[0, 1)$. In other terms, this selection of α_0^X and α_1^X is such that, given p_0^X and p_1^X , there exists a maximum value $\alpha_{\max}^X = \frac{1}{\max(p_0^X, p_1^X)}$ such that (6) holds. This constitutes a lower bound to the average bit-rate of the codeword \mathbf{C}'_X generated by the DAC, i.e. it is not possible to generate a codeword shorter than $H(\mathbf{X}) - \log_2 \alpha_{\max}^X$.

Therefore, we argue that the degrees of freedom in the DAC encoder design could be used to select overlap factors $\alpha_{i,j}^X$ that satisfy (6) by construction. While there are many possible such choices, we have found that the following design performs nicely and has an intuitive interpretation. In particular, we impose that the overlap factors $\alpha_{i,j}^X$ satisfy the following additional constraint:

$$\frac{\delta r_{i,j}^X}{r_{i,j}^X} = k_i^X \quad (7)$$

with k_i^X a positive constant independent of j .

Substituting the definition of $r_{i,j}^X$, $\delta r_{i,j}^X$ into the previous expression, and solving for $\alpha_{i,j}^X$, we obtain

$$\alpha_{i,j}^X = (p_{i,j}^X)^{-k_i^X} \quad (8)$$

which respect the constraint (6), taking $0 \leq k_i^X \leq 1$. Equation (7) can be interpreted as an additional constraint that, at each instant i , the average instantaneous bit-rate saving of DAC with respect to classical AC for the i -th input bit is distributed over the symbols “0” and “1” of the input alphabet depending on their probabilities. In particular, the independence of j means that the amount of bit-rate saving is taken as the same constant fraction of the average instantaneous bit-rate for either symbol “0” or “1”. In terms of amount of information, the least probable symbol requires a higher instantaneous bit-rate, which can be decreased more than the rate of the most probable symbol. In this way we balance the average rate of each symbol of the source alphabet, as determined by its prior probability, and the rate decrease due to the interval overlapping, in such a way that all symbols are treated in the same way. In terms of interval lengths, without overlapping, the least probable symbol has the narrowest interval, and the most probable symbol has the broadest interval. With overlapping, since the interval of the most probable symbol is enlarged less, the non-overlapped portion of the narrowest interval is smaller than the non-overlapped portion of the broadest interval, so that, from the DAC decoder viewpoint, the average amount of ambiguity is the same for either symbol.

D. Derivation of target rate

Using (8), the average coding rate achieved by the DAC can be written as

$$\tilde{R}_k^l(\mathbf{X}) = \frac{1}{l-k+1} \sum_{i=k}^l \sum_{j=0}^1 p_{i,j}^X \left[\log_2 \frac{1}{p_{i,j}^X} - \log_2 \left((p_{i,j}^X)^{-k_i^X} \right) \right] =$$

This can be reworked as

$$\tilde{R}_k^l(\mathbf{X}) = \frac{1}{l-k+1} \sum_{i=k}^l (1 - k_i^X) \sum_{j=0}^1 p_{i,j}^X \log_2 \frac{1}{p_{i,j}^X} = \quad (9)$$

$$= \frac{1}{l-k+1} \sum_{i=k}^l (1 - k_i^X) R_i^i(\mathbf{X}) = \quad (10)$$

where $R_i^i(\mathbf{X})$ is the instantaneous rate achieved by a classical non-distributed AC for the i -th input bit. Finally, the average DAC coding rate can be expressed as the average of these instantaneous rates at time i , each of which is reduced by a factor $1 - k_i^X$.

Comparing Eqs. (1) and (10), the following expression can be obtained for the instantaneous bit-rate of the DAC, as a function of the equivalent instantaneous rate of an AC:

$$\tilde{R}_i^i(\mathbf{X}) = (1 - k_i^X) R_i^i(\mathbf{X}) \quad (11)$$

This shows that one way to achieve the target bit-rate is to allocate the rate bit by bit, based on the probability mass function at each instant i . Given the probabilities $p_{i,0}^X$ and $p_{i,1}^X$, which in turn determine $R_i^i(\mathbf{X})$, and the target instantaneous rate $\tilde{R}_i^i(\mathbf{X})$, (11) can be solved for k_i^X . The statistical modeler has to find a proper way to subdivide the total target bit-rate $\tilde{R}_k^l(\mathbf{X})$ into $l - k + 1$ contributions $\tilde{R}_i^i(\mathbf{X})$. Two factors come into play in this subdivision, i.e. whether the source is stationary, and hence $p_{i,0}^X$ and $p_{i,1}^X$ do not depend on i , and whether the correlation of the source is also stationary. Both factors contribute to the selection of the proper rate for each index i . Intuitively, a source with small entropy should be allocated a smaller rate than a source with high entropy. On the other hand, the rate should generally be higher if the source and the side information are not very correlated at index i . These two aspects are reflected by the two terms $R_i^i(\mathbf{X})$ and $(1 - k_i^X)$ of (11), which account respectively for the source entropy and the correlation with the side information.

In more general terms, looking at (10) globally and not bit by bit, it can be seen that the allocation problem where one has to select a set of coefficients k_i^X , $i = 0, \dots, N - 1$ so as to achieve a target rate $\tilde{R}_0^{N-1}(\mathbf{X})$, is underdetermined. Indeed, given the prior probabilities $p_{i,j}^X$, we have one equation and N unknowns k_i^X ; as a consequence, any set of coefficients k_i^X that satisfy the equation above will generate a codeword whose average length is as desired. However, it should be noted that not all set of coefficients k_i^X are equally good from the DAC decoder standpoint. For example, let us consider a source that emits two symbols ($N = 2$), with probability distribution independent of i ; moreover, let us assume that the first symbol X_0 is extremely correlated with the side information Y_0 , while the second symbol X_1 is weakly correlated with Y_1 . It is intuitive that, although the average instantaneous rate for X_0 and X_1 is the same, i.e. $R_0^0(\mathbf{X}) = R_1^1(\mathbf{X})$, the DAC encoding process should allocate more ambiguity to X_0 than X_1 , because the side information carries more information on X_0 than X_1 . As a consequence, the value of k_i^X should be set bit by bit based on the prior probabilities and the correlation with the side information.

In particular, we define N allocation problems in the form $\tilde{R}_i^i(\mathbf{X}) = (1 - k_i^X) R_i^i(\mathbf{X})$, with $i = 0, \dots, N - 1$, subject to the constraint that $\sum_{i=0}^{N-1} \tilde{R}_i^i(\mathbf{X}) = R'_X$. We assume that a set of conditional entropies $H(X_i|Y_i)$ is available as in Fig. 4, modeling the correlation between \mathbf{X} and \mathbf{Y} . In asymmetric

DSC, \mathbf{X} should be ideally coded at a rate arbitrarily close to $H(\mathbf{X}|\mathbf{Y})$. In practice, due to the suboptimality of any practical coder, some margin $\mu \geq 1$ should be taken; hence, we assume that the i -th allocation problem can be written as $\mu H(X_i|Y_i) = (1 - k_i^X) R_i^i(\mathbf{X})$. Since μ is a constant, $H(X_i|Y_i)$ is given, and $R_i^i(\mathbf{X})$ is fixed once the prior probabilities $p_{i,j}^X$ are given, one can solve for k_i^X and then perform the encoding process.

E. A few special cases

Although so far the notation has been kept very general, particularly regarding the dependence on i , a few special cases can be identified, which are important for practical applications, and for which the rate allocation problem can be simplified.

The special case $k_i^X = 0$ for all i represents a classical, non distributed AC, which does not perform any interval overlapping, and achieves a coding rate equal to

$$\tilde{R}_k^l(\mathbf{X}) = R_k^l(\mathbf{X}) = \frac{1}{l - k + 1} \sum_{i=k}^l \sum_{j=0}^1 p_{i,j}^X \log_2 \frac{1}{p_{i,j}^X}$$

Another special case is particularly interesting, i.e. when the source \mathbf{X} is identically distributed, and the correlation between X_i and Y_i is stationary (i.e., $H(X_i|Y_i)$ does not depend on i). This occurs for example when \mathbf{X} is an i.i.d. process, and \mathbf{Y} is derived from \mathbf{X} through a memoryless transformation; e.g., \mathbf{Y} can be obtained as the output of a binary symmetric channel with crossover probability p . The first condition implies that the probabilities $p_{i,j}^X$ are independent of i , and can be written as $p_{i,0}^X = p_0^X$ and $p_{i,1}^X = p_1^X$. The second condition allows to choose $k_i^X = k^X \forall i$. Therefore, the expression of the average coding rate can be further simplified as

$$\tilde{R}_k^l(\mathbf{X}) = (1 - k^X) \sum_{j=0}^1 p_j^X \log_2 \frac{1}{p_j^X} = (1 - k^X) H(\mathbf{X}).$$

Another interesting case occurs when context-based coding takes place, i.e. when each sample of the source can be modeled as belonging to one out of a given number C of contexts \mathcal{C}_w , $w = 0, \dots, C-1$. Inside each context \mathcal{C}_w , the source can be modeled as an i.i.d. source with probabilities $p_{(w),0}^X$ and $p_{(w),1}^X$ that do not depend on i . Let us denote as \mathcal{R}_w the set of all indexes i such that X_i belongs to context \mathcal{C}_w , i.e. $\mathcal{R}_w = \{i : X_i \in \mathcal{C}_w\}$. We also assume that, within each context, the correlation with the side information is stationary, i.e. $H(X_i|Y_i) = \bar{H}_w \forall i \in \mathcal{R}_w$. Then, the target rate R'_X can be written as

$$R'_X = \tilde{R}_0^{N-1}(\mathbf{X}) = \frac{1}{N} \sum_{w=0}^{C-1} |\mathcal{R}_w| \left(1 - k_{(w)}^X\right) H_w(\mathbf{X}) \quad (12)$$

with $|\mathcal{R}_w|$ the cardinality of \mathcal{R}_w , and $H_w(\mathbf{X}) = -\sum_{j=0}^1 p_{(w),j}^X \log_2 p_{(w),j}^X$ the entropy of the i.i.d. model inside context \mathcal{C}_w . The rate allocation problem can be separated into w problems, one per

context, where one solves for DAC parameter $k_{(w)}^X$, to be used for all $i \in \mathcal{R}_w$, such that

$$\mu \bar{H}_w = \frac{|\mathcal{R}_w|}{N} \left(1 - k_{(w)}^X\right) H_w(\mathbf{X})$$

IV. DISTRIBUTED ARITHMETIC CODING: DECODER

The objective of the distributed arithmetic decoder is joint decoding of the source message \mathbf{X} given the correlated side information \mathbf{Y} . The decoding process can be formulated as a symbol-driven sequential search along a proper decoding tree, where each node represents a state of the sequential arithmetic decoder. Transitions between different states are driven by a suitable metric; for DAC, we employ the *Maximum A Posteriori* (MAP) metric $P(\mathbf{X}|\mathbf{C}'_X, \mathbf{Y})$. The decoder operates as follows; the number of symbols N is assumed to be known.

Algorithm 1 DAC decoder

```

Initialize the sequential AC decoder and store its state as the root node of the decoding tree
Set symbol counter  $i \leftarrow 0$ 
Subdivide the interval according to the probabilities  $\tilde{p}_{i,j}$ 
while The number of decoded symbols is less than  $N$  ( $i < N$ ) do
  for All the nodes in the tree do
    Compare  $\mathbf{C}'_X$  with the current interval subdivisions.
    if  $\mathbf{C}'_X$  belongs to the non overlapped portion of a certain interval then
      Decode the corresponding symbol  $X_i$  without ambiguity and select the corresponding
      interval for next iteration of this node
      Update MAP metric of the node
    else
      Perform a decoding branching
      Store two alternative nodes in memory, i.e. two AC decoder states, corresponding to the
      two alternative symbols  $X_i$  that can be decoded
      Update their MAP metrics and select the corresponding interval for next iteration
    end if
  end for
  Prune the decoding tree by keeping only the  $M$  most likely paths (M algorithm)
end while
Output the sequence corresponding to the most likely path, survived in the tree.

```

Fig. 5 depicts a decoder branching; in particular, in this example the decoder is not able to make a

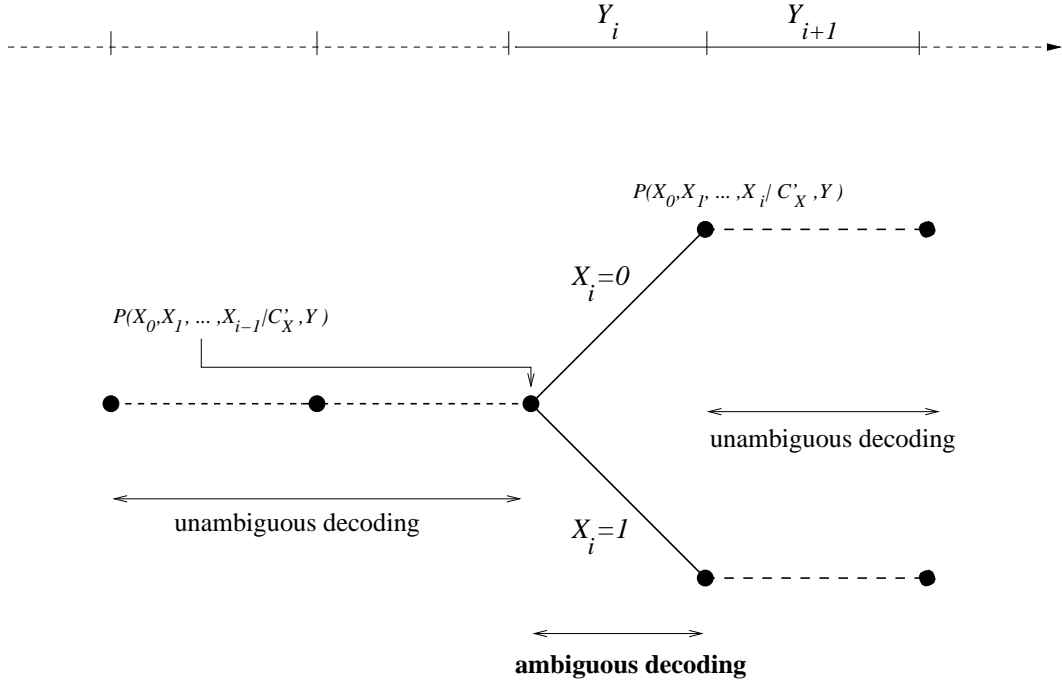


Fig. 5. Distributed arithmetic decoding tree for asymmetric S-W coding.

decision on the i -th symbol X_i . As a consequence, two alternative decoding attempts are pursued. On one branch, the $X_i = 0$ hypothesis is considered and the MAP metric $P(X_0, X_1, \dots, X_i = 0 | \mathbf{C}'_X, \mathbf{Y})$ is updated accordingly. On the other branch the opposite decision is considered, and the MAP metric $P(X_0, X_1, \dots, X_i = 1 | \mathbf{C}'_X, \mathbf{Y})$ is evaluated. In general, there will be a certain number of ambiguous positions i , yielding a tree of decoder states that must be visited by the sequential search algorithm seeking the most likely solution.

Given the correlation model in terms of the probability distribution $P(\mathbf{X}|\mathbf{Y})$, the MAP metric can be evaluated iteratively as

$$P(X_0, X_1, \dots, X_i | \mathbf{C}'_X, \mathbf{Y}) = P(X_0, X_1, \dots, X_{i-1} | \mathbf{C}'_X, \mathbf{Y}) P(X_i | \mathbf{C}'_X, \mathbf{Y})$$

with $P(X_i | \mathbf{C}'_X, \mathbf{Y}) = P(X_i | \mathbf{Y})$. We adopt a memoryless correlation model with $P(\mathbf{X}|\mathbf{Y}) = \prod_{i=0}^{N-1} P(X_i | Y_i)$. The last term of the MAP metric can be then simplified as $P(X_i | \mathbf{C}'_X, Y_i) = P(X_i | Y_i)$. The same approach can be extended to correlation models with memory with proper adaptation of the branch metric.

It is worth noticing that most applications will adopt a logarithmic implementation of the previous metrics so as to substitute multiplications with additions. As far as tree pruning, possible techniques are the Viterbi, stack, and M algorithms (see e.g. [32]). In the present implementation of Algorithm 1 we adopt the M algorithm for tree pruning, thus only the M nodes, which exhibit the best metrics

at each iteration i are stored for future recursions. M shall be selected as a trade-off between memory/complexity cost and the probability that the path corresponding to the encoded sequence \mathbf{X} is accidentally dropped. As in the case of standard Viterbi decoding, the path metric turns out to be stable and reliable as long as a significant amount of terms, i.e. number of decoded symbols X_i , are taken into account. In the pessimistic case when all symbol positions i trigger a decoder branching, given M , one can guarantee that at least $\log_2(M)$ symbols are considered for metric comparisons and pruning. On the other hand, in practical cases, the interval overlap is only partial and branching does not occur at every symbol iteration. In practice, we have empirically found that $M = 2048$ is a good compromise between metric stability and complexity; this value has been used for all the experimental results presented in Sect. V.

Finally, metric reliability cannot be guaranteed for the very last symbols of a finite length sequence \mathbf{X} ; for channel codes, e.g. convolutional codes, this issue is tackled by imposing a proper termination strategy, e.g. forcing the encoded sequence to end in the first state of the trellis. A similar approach is necessary when using DAC. Examples of AC termination strategies are the encoding of a known termination pattern or end-of-block symbol with a certain probability or, in the case of context-based AC, the driving of the AC encoder in a given context. For DAC, we employ a new termination policy that is tailored to its particular features. Termination is obtained by encoding the last T symbols of the source block without interval overlap, i.e. $\tilde{p}_{i,j}^X = p_{i,j}^X$, for $i \geq N - T$. As a consequence, all the nodes in the DAC decoding tree will not cause branching in the last T steps, making the final metrics more reliable for the selection of the most likely sequence. Using the notation defined in Sect.III, the overall coding rate yielded by DAC in presence of termination turns out to be:

$$R_T(\mathbf{X}) = \sum_{i=0}^{N-T-1} \tilde{R}_i^i(\mathbf{X}) + \sum_{i=N-T}^{N-1} R_i^i(\mathbf{X}) \quad (13)$$

The rate penalty incurred by the termination policy depends on the number of terminating symbols T and their rate cost $R_i^i(\mathbf{X}) \geq \tilde{R}_i^i(\mathbf{X})$.

V. RESULTS

In the following we provide results of a performance evaluation carried out on DAC. We implement a communication system that employs a DAC and a soft joint decoder, with no feed-back channel; at the decoder, pruning is performed using the M-algorithm [32], with $M=2048$. The side information is obtained by sending the sequence \mathbf{X} through a binary symmetric channel with transition probability p , which measures the correlation between the two sources. Unless otherwise specified, each point of the figures/tables presented in the following has been generated averaging the results obtained encoding 10^7 samples.

A. Effect of termination

As a first experiment, the benefit of the termination policy is assessed. An i.i.d. stationary source of $N = 200$ symbols with $p_0 = 0.5$ and side information correlated such that $H(\mathbf{X}|\mathbf{Y}) = 0.25$, is encoded with DAC at 0.5 bps, i.e. 0.25 bps higher than the theoretical S-W bound. The bit error rate (BER) yielded by the decoder is measured for increasing values of the number of termination symbols T . The same simulation is performed with $N = 1000$. In all simulated cases, the DAC overlap has been selected to compensate for the rate penalty incurred by the termination, inverting (13) so as to achieve the 0.5 bps overall target rate. The overlap factors $\alpha_{i,j}^X$ are selected according to (8).

The results are shown in Fig. 6; it can be seen that the proposed termination is effective at reducing the BER. There is a trade-off in that, for a given bit-rate, increasing T reduces the effect of errors in the last symbols, but requires to overlap the intervals more. The optimal values of T are around 15-20 symbols. Therefore, we have selected $T = 15$ and used this value for all the experiments reported in the following.

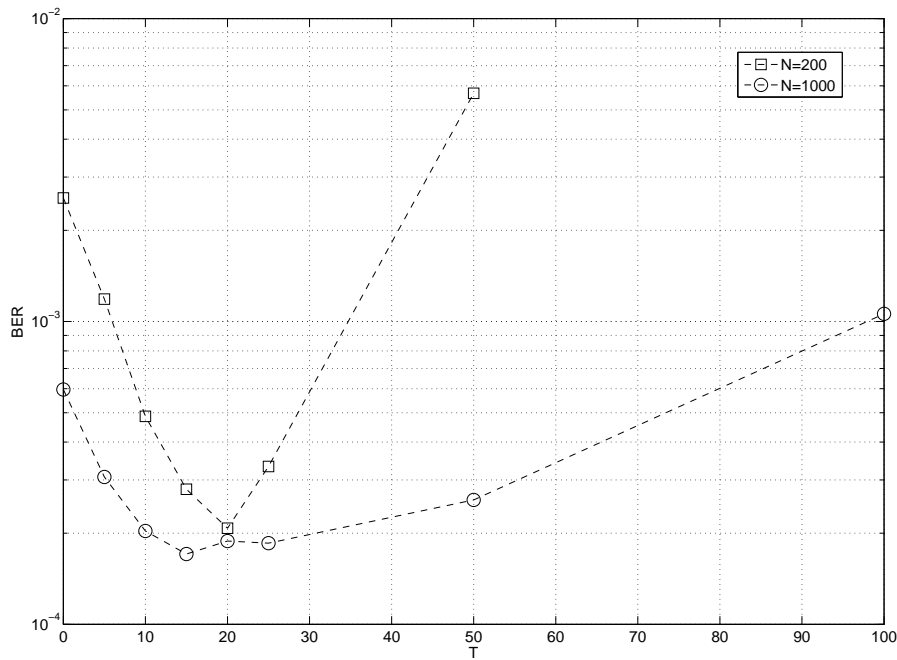


Fig. 6. BER as function of T (number of termination symbols); $p_0 = 0.5$, total rate = 1.5 bps, $H(\mathbf{X}|\mathbf{Y}) = 0.25$.

B. Effect of the overlap design rule

Next, an experimental validation of the theoretical analysis of the effects of different overlap designs shown in Sect. III-B, is provided. In Fig. 7 the performance obtained by using the design of equations

(5) and (8) respectively is shown. The experimental settings are $N = 200$, $p_0 = 0.8$, total coding rate $R_X + R_Y = 1$ bps. BER and frame error rate (FER) are reported as a function of the source correlation expressed in terms of $H(\mathbf{X}, \mathbf{Y})$. It is worth noticing that the performance yielded by different overlap design rules are almost overlapped, as predicted by theory.

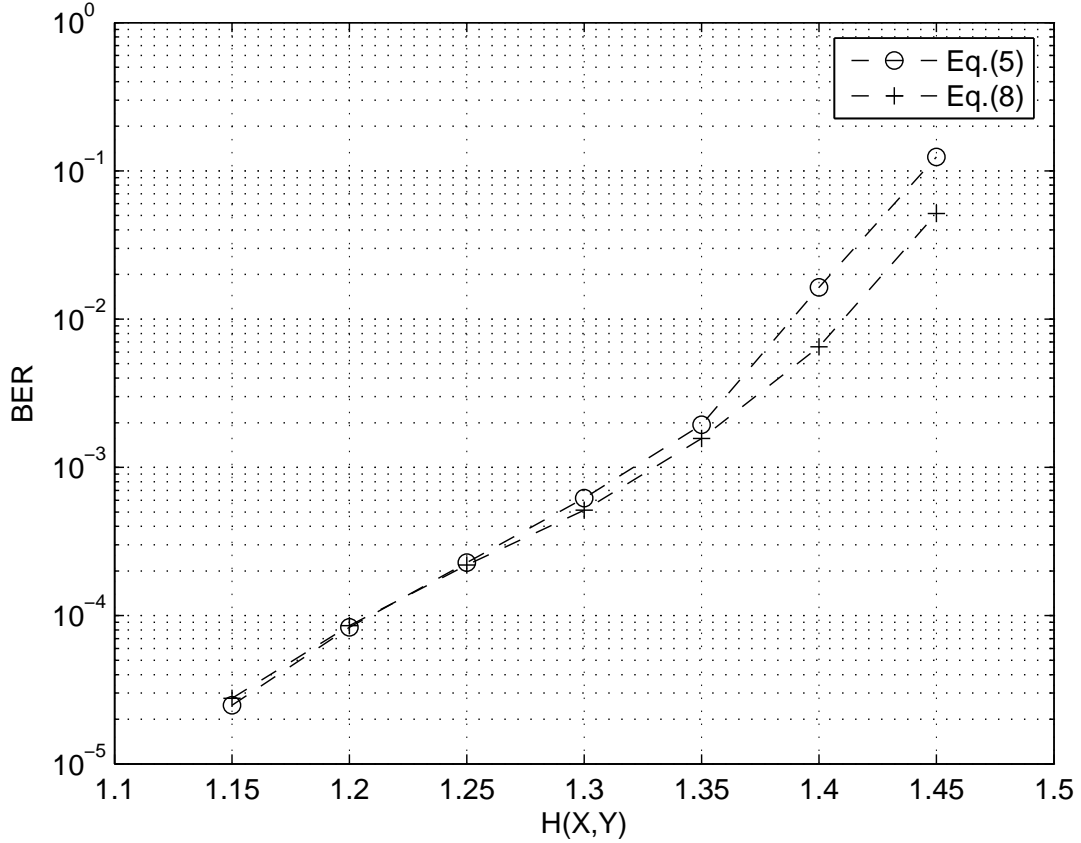


Fig. 7. Performance comparison between the use of linear and logarithmic overlap ($p_0 = 0.5$, total rate = 1.5 bps).

C. Performance evaluation at fixed rate

The performance of the proposed system is compared with that of a system where the DAC encoder and decoder are replaced by a punctured turbo code similar to that in [6]; we use turbo codes with rate- $\frac{1}{2}$ generator (17,15) octal (8 states) and (31,27) octal (16 states), and employ S-random interleavers, and 15 decoder iterations. We consider the case of symmetric source ($p_0 = p_1 = 0.5$) and asymmetric source (in particular $p_0 = 0.9$ and $p_0 = 0.8$); for an asymmetric source, as an improvement with respect to [6], the turbo decoder has been modified by adding to the decoder metric the *a priori* term, as done in [16]. Block sizes $N = 50$, $N = 200$ and $N = 1000$ have been considered (with S-random

interleaver spread of 5, 11 and 25 respectively); this allows to assess the DAC performance at small and medium block lengths. Besides turbo codes, we also considered the rate-compatible LDPC codes proposed in [21]. For these codes, a software implementation is publicly available on the web; among the available pre-designed codes, we used the matrix for $N = 396$, which is comparable with the block sizes considered for the DAC and the turbo code.

The results are worked out in a fixed-length coding setting as in [14], i.e. the coding rate is the same for each sample realization of the source. Fig. 8 reports the results for the symmetric source case; the abscissa $H(\mathbf{X}|\mathbf{Y})$ is the conditional entropy of the source given the side information, and is related to p . The higher p , the less correlated the sources, and hence the higher $H(\mathbf{X}|\mathbf{Y})$. The performance is measured in terms of the residual BER after decoding, which is akin to the distortion in the Wyner-Ziv binary coding problem with Hamming distortion metric. Both the DAC and the turbo code generate a description of \mathbf{X} of size $N/2$ bits, achieving a 2:1 compression ratio; the total bit-rate of \mathbf{X} and \mathbf{Y} is 1.5 bps. Since $H(\mathbf{Y}) = 1$, we also have that $H(\mathbf{X}, \mathbf{Y}) = 1 + H(\mathbf{X}|\mathbf{Y})$; this makes it possible to compare these results with the case of asymmetric sources which is presented later in this section.

As can be seen, the performance of DAC slightly improves as the block length increases. This is mostly due to the effect of the termination. As the number of bits used to terminate the encoder is chosen independently of the block length, the rate penalty for non overlapping the last bits weights more when the block length is small, while the effect vanishes for large block length. In [27], where the termination effect is not considered, the performance is shown to be almost independent of the block size. It should also be noted that the decoder memory required for near-optimal performance grows exponentially with the block size. As a consequence, the memory which leads to near-optimal performance for $N = 50$ or $N = 200$ limits the performance for $N = 1000$. This is also a reason why the DAC performance is little dependent on the block length.

We compared both 8-states and 16-states turbo codes; the 8-states code is often used in practical applications, as it exhibits a good trade-off between performance and complexity; the 16-states code is more powerful, and requires more computations. It can be seen that, for block length $N = 50$ and $N = 200$, the proposed system outperforms the 8-states and 16-states turbo codes. For block length $N = 1000$, the DAC performs better than the 8-states turbo code, and is equivalent to the 16-states code. It should be noted that, in this experiment, only the “channel coding performance” of the DAC is tested, since for the symmetric source no compression is possible ($H(\mathbf{X}) = 1$); consequently, it is remarkable that the DAC turns out to be generally more powerful than the turbo code at equal block length. Note that the performance of the 16-states code is limited by the error floor, and could be improved using an ad-hoc design of the code or the interleaver; the DAC has no error floor, but

its waterfall is less steep. For $H(\mathbf{X}|\mathbf{Y}) \geq 0.35$, a result not reported in Fig. 8 shows that the DAC with $N = 200$ and $N = 1000$ also outperform the 8-state turbo-coder with $N = 5000$. In terms of the rate penalty, setting a residual BER threshold of 10^{-4} , for $N = 200$ the DAC is almost 0.3 bps away from the S-W limit, while the best 16-state turbo code simulated in this paper is 0.35 bps away; for $N = 1000$ the DAC is 0.26 bps away, while the best 8-state turbo code is 0.30 bps away. The performance of the LDPC code for $N = 396$ is halfway between the turbo codes for $N = 200$ and $N = 1000$, and hence very similar to the DAC.

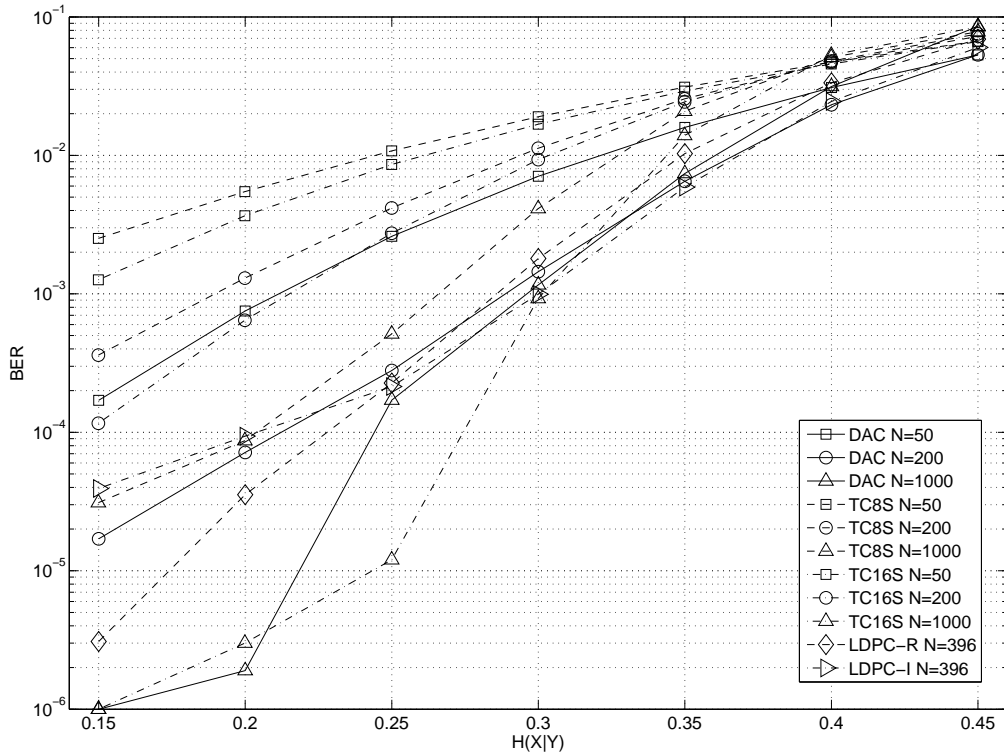


Fig. 8. Performance comparison of data communication systems ($p_0 = 0.5$, total rate = 1.5 bps): distributed arithmetic coding versus turbo coding, symmetric source. DAC: distributed arithmetic coding; TC8S and TC16S: 8- and 16-state turbo code with S-random interleaver; LDPC-R and LDPC-I: regular and irregular LDPC codes from [21].

The results for an asymmetric source are reported in Fig. 9 for $p_0 = 0.8$. In this setting, we select various values of $H(\mathbf{X}, \mathbf{Y})$, and encode \mathbf{X} at rate $1 - H(\mathbf{Y})$, with a total rate budget of 1.5 bps. Consistently with [33], all turbo codes considered in this work perform rather poorly on asymmetric sources. In [33] this behavior is explained with the fact that, when the source is asymmetric, the states of the turbo code are used with uneven probability, leading to a smaller equivalent number of states. On the other hand, the DAC has good performance also for asymmetric sources, as it is designed

to work with unbalanced distributions. The performance of the LDPC codes is similar to that of the best turbo codes, and slightly worse than the DAC.

Similar remarks can be made in the case of $p_0 = 0.9$, whose results are reported in Fig. 10. For this case, we have selected a total rate of 1 bps, since the source is more unbalanced and hence easier to compress. In this case the turbo code performance is better than in the previous case. This is due to the fact that the sources are more correlated, and hence the crossover probability on the virtual channel is lower. Therefore, the turbo code has to correct a smaller number of errors, whereas in the $p_0 = 0.8$ case the correlation was weaker and hence the crossover probability was higher.

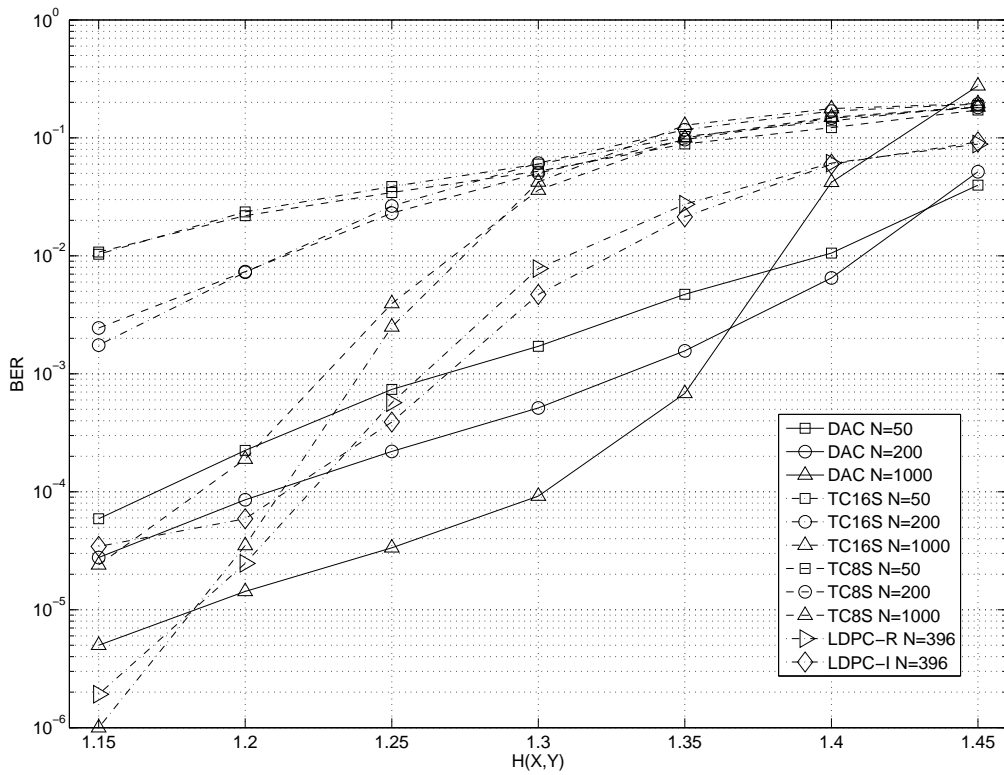


Fig. 9. Performance comparison of data communication systems ($p_0 = 0.8$, total rate = 1.5 bps): distributed arithmetic coding versus turbo coding, asymmetric source. DAC: distributed arithmetic coding; TC8S and TC16S: 8- and 16-state turbo code with S-random interleaver; LDPC-R and LDPC-I: regular and irregular LDPC codes from [21].

D. Performance evaluation for very correlated sources

We also considered the case of extremely correlated sources, for which high-rate channel codes are needed. These sources are a good model for the most significant bit-planes of several multimedia

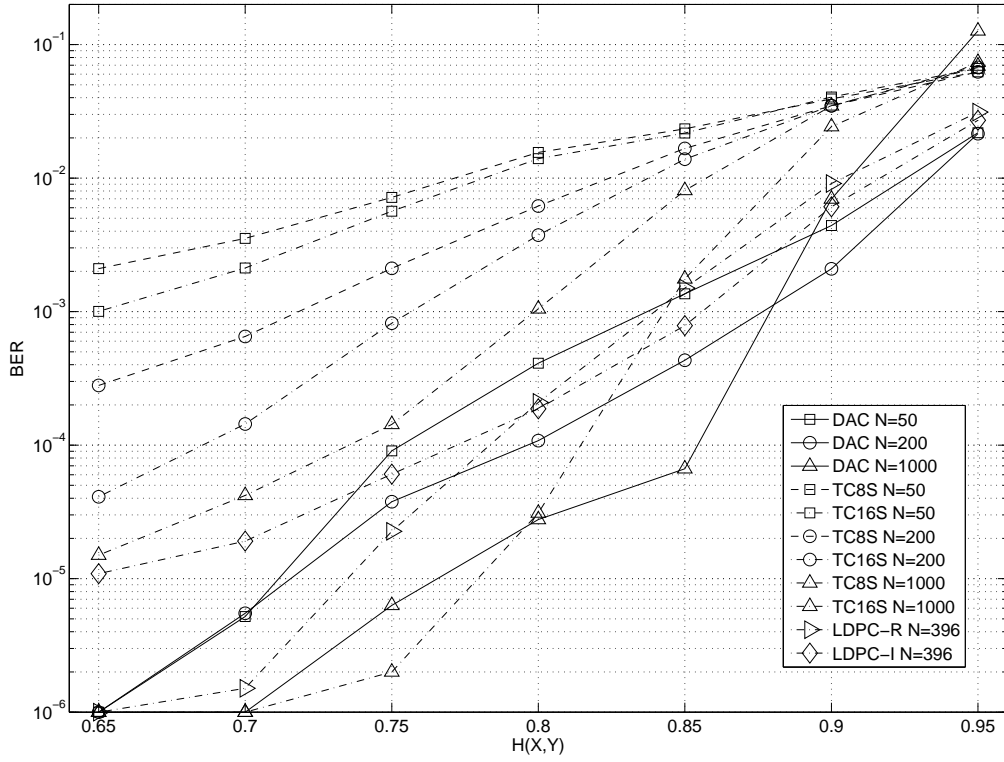


Fig. 10. Performance comparison of data communication systems ($p_0 = 0.9$, total rate = 1 bps): distributed arithmetic coding versus turbo coding, asymmetric source. DAC: distributed arithmetic coding; TC8S and TC16S: 8- and 16-state turbo code with S-random interleaver; LDPC-R and LDPC-I: regular and irregular LDPC codes from [21].

signals; due to the inefficiency of syndrome-based coders, practical schemes often assume that no DSC is carried out on those bit-planes, e.g. they are not transmitted, and at the decoder they are directly replaced by the side information [9].

The results are reported in Tab. I for the DAC and the 16-state turbo code. As can be seen, the DAC has similar performance to the turbo codes and LDPC codes, and becomes better when the source is extremely correlated, i.e. $H(\mathbf{X}|\mathbf{Y}) = 0.001$.

E. Performance evaluation at variable rate

Finally, the coding efficiency of DAC is measured in terms of average coding rate required to achieve error-free decoding. This amounts to re-encoding the source at increasing rates, and represents the optimal DAC performance if the encoder could exactly predict the decoder behavior. Since each realization of the source is encoded using a different number of bits, this case is referred to as variable-length encoding. This scenario is representative of practical distributed compression settings,

TABLE I

RESIDUAL BER IN CASE OF VERY CORRELATED SOURCES, WITH $p_0 = 0.5$ AND 10:1 COMPRESSION RATIO

$N = 200$		
$H(\mathbf{X} \mathbf{Y})$	DAC	TC16S
0.1	$2.25 \cdot 10^{-2}$	$1.05 \cdot 10^{-2}$
0.01	$2.55 \cdot 10^{-4}$	$1.74 \cdot 10^{-4}$
0.001	$1.5 \cdot 10^{-6}$	$7.0 \cdot 10^{-6}$
$N = 1000$		
$H(\mathbf{X} \mathbf{Y})$	DAC	TC16S
0.1	$2.10 \cdot 10^{-2}$	$1.18 \cdot 10^{-2}$
0.01	$1.5 \cdot 10^{-5}$	$2.9 \cdot 10^{-5}$
0.001	$< 1 \cdot 10^{-6}$	$1.0 \cdot 10^{-6}$
$N = 396$		
$H(\mathbf{X} \mathbf{Y})$	LDPC-R	LDPC-I
0.1	$1.20 \cdot 10^{-2}$	$1.11 \cdot 10^{-2}$
0.01	$1.18 \cdot 10^{-4}$	$1.01 \cdot 10^{-4}$
0.001	$4.65 \cdot 10^{-6}$	$7.58 \cdot 10^{-6}$

e.g. [6], in which one seeks the shortest code that allows to reconstruct without errors each realization of the source process.

For this simulation, the following setup is used. The source correlation $H(\mathbf{X}|\mathbf{Y})$ is kept constant and, for each sample realization of the source, the total coding rate is progressively increased beyond the S-W bound until error-free decoding is obtained. This operation is repeated on 1000 different realizations of the source; the average of the rates yielding correct decoding is then computed.

The results have been worked out for block length $N = 200$, with probabilities $p_0 = 0.5$ and $p_0 = 0.9$. For $p_0 = 0.5$, the conditional entropy $H(\mathbf{X}|\mathbf{Y})$ (i.e. the S-W bound) has been set to 0.5 bps. For $p_0 = 0.9$, the joint entropy $H(\mathbf{X}, \mathbf{Y})$ has been set to 1 bps; this amounts to coding \mathbf{Y} at the ideal rate of $H(\mathbf{Y}) \simeq 0.715$ bps, with a S-W bound $H(\mathbf{X}|\mathbf{Y}) \simeq 0.285$ bps.

The results are reported in Tab. II. As can be seen, the DAC as a rate loss of about 0.06 bps with respect to the S-W bound for both the symmetric and asymmetric source. The turbo code exhibits a loss of about 0.2 bps and 0.13 bps. The LDPC-R code has a relatively small loss, i.e. 0.12 bps in the symmetric case and 0.10 in the asymmetric one. The LDPC-I code has a slightly smaller loss, i.e. 0.09 bps in the symmetric case and 0.075 in the asymmetric one. However, the DAC still performs slightly better.

TABLE II
PERFORMANCE COMPARISON FOR VARIABLE-RATE CODING.

	$p_0 = 0.5$	$p_0 = 0.9$
$H(\mathbf{X} \mathbf{Y})$	0.50	0.275
DAC $N = 200$	0.56	0.32
LDPC-R $N = 396$	0.62	0.37
LDPC-I $N = 396$	0.59	0.35
TC16S $N = 200$	0.71	0.42
TC16S $N = 1000$	0.70	0.41

VI. DISCUSSION AND CONCLUSIONS

We have proposed DAC as an alternative to existing DSC coders based on channel coding.

DAC achieves good compression performance, comparable with or better than that of turbo and LDPC codes at small and medium block lengths; this is very important in many applications, e.g. in the multimedia field, where the encoder partitions the compressed file into small units (e.g. packets in JPEG 2000, slices and NALUs in H.264/AVC) that have to be coded independently.

As for encoding complexity, which is of great interest for DSC, DAC has linear encoding complexity, like a classical AC [34]. Turbo codes and the LDPC codes in [21] also have linear encoding complexity, whereas general LDPC codes typically have more than linear, and typically quadratic complexity [35]. As a consequence, the complexity of DAC is suitable for DSC applications.

A major advantage of DAC lies in the fact that it can exploit statistical prior knowledge about the source very easily. This is a strong asset of ACs, which is retained by DAC. Probabilities can be estimated on-the-fly based on past symbols; context-based models employing conditional probabilities can also be used, as well as other models providing the required probabilities. These models allow to account for the nonstationarity of typical real-world signals. This is a significant advantage over DSC coders based on channel codes, as these coders are designed assuming a stationary signal model over the whole block, and hence cannot take proper advantage of prior information.

Another advantage of the proposed DAC lies in the fact that the encoding process can be seen as a simple extension of the AC process. As a consequence, it is straightforward to extend an existing scheme employing AC as final entropy coding stage in order to provide DSC functionalities.

REFERENCES

- [1] D. Slepian and J.K. Wolf, "Noiseless coding of correlated information sources," *IEEE Transactions on Information Theory*, vol. 19, pp. 471–480, July 1973.

- [2] A. Wyner and J. Ziv, "The rate-distortion function for source coding with side information at the decoder," *IEEE Transactions on Information Theory*, vol. 22, pp. 1–10, Jan. 1976.
- [3] S.S. Pradhan, J. Chou, and K. Ramchandran, "Duality between source coding and channel coding and its extension to the side information case," *IEEE Transactions on Information Theory*, vol. 49, no. 5, pp. 1181–1203, May 2003.
- [4] R. Zamir, "The rate loss in the Wyner-Ziv problem," *IEEE Transactions on Information Theory*, vol. 42, no. 6, pp. 2073–2084, Nov. 1996.
- [5] R. Puri and K. Ramchandran, "PRISM: a "reversed" multimedia coding paradigm," in *Proc. of IEEE International Conference on Image Processing*, 2003.
- [6] B. Girod, A. Aaron, S. Rane, and D. Rebollo-Monedero, "Distributed video coding," *Proceedings of the IEEE*, vol. Special Issue on Advances in Video Coding and Delivery, no. 1, pp. 71–83, Jan. 2005.
- [7] M. Grangetto, E. Magli, and G. Olmo, "Context-based distributed wavelet video coding," in *Proceedings of IEEE International Workshop on Multimedia Signal Processing*, 2005.
- [8] C. Guillemot, F. Pereira, L. Torres, T. Ebrahimi, R. Leonardi, and J. Ostermann, "Distributed monoview and multiview video coding," *IEEE Signal Processing Magazine*, vol. 24, no. 5, pp. 67–76, Sept. 2007.
- [9] Q. Xu and Z. Xiong, "Layered Wyner-Ziv video coding," *IEEE Transactions on Image Processing*, vol. 15, no. 12, pp. 3791–3803, Dec. 2006.
- [10] H. Wang and A. Ortega, "Scalable predictive coding by nested quantization with layered side information," in *Proceedings of IEEE International Conference on Image Processing*, 2004.
- [11] A. Sehgal, A. Jagmohan, and N. Ahuja, "Wyner-Ziv coding of video: an error-resilient compression framework," *IEEE Transactions on Multimedia*, vol. 6, no. 2, pp. 249–258, Apr. 2004.
- [12] E. Magli, M. Barni, A. Abrardo, and M. Grangetto, "Distributed source coding techniques for lossless compression of hyperspectral images," *EURASIP Journal on Advances in Signal Processing*, vol. 2007, 2007.
- [13] N.-M. Cheung, C. Tang, A. Ortega, and C.S. Raghavendra, "Efficient wavelet-based predictive Slepian-Wolf coding for hyperspectral imagery," *Signal Processing*, vol. 86, no. 11, pp. 3180–3195, Nov. 2006.
- [14] Z. Xiong, A.D. Liveris, and S. Cheng, "Distributed source coding for sensor networks," *IEEE Signal Processing Magazine*, vol. 21, no. 5, pp. 80–94, Sept. 2004.
- [15] S.S. Pradhan and K. Ramchandran, "Distributed source coding using syndromes (DISCUS): Design and construction," *IEEE Transactions on Information Theory*, vol. 49, no. 3, pp. 626–643, Mar. 2003.
- [16] J. Garcia-Frias and Y. Zhao, "Compression of correlated binary sources using turbo codes," *IEEE Communications Letters*, vol. 5, no. 10, pp. 417–419, Oct. 2001.
- [17] A.D. Liveris, Z. Xiong, and C.N. Georgiades, "Distributed compression of binary sources using conventional parallel and serial concatenated convolutional codes," in *Proc. of IEEE Data Compression Conference*, 2003.
- [18] R. Gallager, *Low Density Parity Check Codes*, MIT Press, 1963.
- [19] A. Liveris, Z. Xiong, and C. Georgiades, "Compression of binary sources with side information at the decoder using LDPC codes," *IEEE Communications Letters*, vol. 6, pp. 440–442, Oct. 2002.
- [20] Y. Yang, S. Cheng, Z. Xiong, and W. Zhao, "Wyner-Ziv coding based on TCQ and LDPC codes," in *Proceedings of Asilomar Conference on Signals, Systems, and Computers*, 2003.
- [21] D. Varodayan, A. Aaron, and B. Girod, "Rate adaptive codes for distributed source coding," *Signal Processing*, vol. 86, no. 11, pp. 3123–3130, Nov. 2006.
- [22] Z. Tu, J. Li, and R.S. Blum, "Compression of a binary source with side information using parallelly concatenated convolutional codes," in *Proceedings of IEEE GLOBECOM*, 2004.
- [23] A. Majumdar, J. Chou, and K. Ramchandran, "Robust distributed video compression based on multilevel coset codes," in *Proceedings of Thirty-Seventh Asilomar Conference on Signals, Systems and Computers*, 2003.

- [24] S. Cheng and Z. Xiong, "Successive refinement for the Wyner-Ziv problem and layered code design," *IEEE Transactions on Signal Processing*, vol. to appear.
- [25] P. Koulgi, E. Tuncel, S.L. Regunathan, and K. Rose, "On zero-error source coding with decoder side information," *IEEE Transactions on Information Theory*, vol. 49, no. 1, pp. 99–111, Jan. 2003.
- [26] Q. Zhao and M. Effros, "Lossless and near-lossless source coding for multiple access networks," *IEEE Transactions on Information Theory*, vol. 49, no. 1, pp. 112–128, Jan. 2003.
- [27] M. Grangetto, E. Magli, and G. Olmo, "Distributed arithmetic coding," *IEEE Communications Letters*, vol. 11, no. 11, pp. 883–885, Nov. 2007.
- [28] X. Artigas, S. Malinowski, C. Guillemot, and L. Torres, "Overlapped quasi-arithmetic codes for distributed video coding," in *Proceedings of IEEE ICIP*, 2007.
- [29] J. Li, Z. Tu, and R.S. Blum, "Slepian-Wolf coding for nonuniform sources using turbo codes," in *Proceedings of IEEE Data Compression Conference*, 2004.
- [30] M. Grangetto, E. Magli, and G. Olmo, "Symmetric distributed arithmetic coding of correlated sources," in *Proceedings of IEEE MMSP*, 2007.
- [31] T. M. Cover and J. A. Thomas, *Elements of Information Theory*, Wiley, New York, 1991.
- [32] J.B. Anderson and S. Mohan, *Source and Channel Coding*, Kluwer, 1991.
- [33] P. Tan and J. Li, "A general and optimal framework to achieve the entire rate region for Slepian-Wolf coding," *Signal Processing*, vol. 86, no. 11, pp. 3102–3114, Nov. 2006.
- [34] H. Helfgott, "Linear-time construction of optimal context trees," in *Proceedings of IEEE Data Compression Conference*, 1998.
- [35] T.J. Richardson and L.R. Urbanke, "Efficient encoding of low-density parity-check codes," *IEEE Transactions on Information Theory*, vol. 47, no. 2, pp. 638–656, Feb. 2001.

